FRP DEBONDING PREVENTION OF STRENGTHENED CONCRETE MEMBERS UNDER DYNAMIC LOAD USING SMART PIEZOELECTRIC MATERIALS (PZT)

M. E. Voutetaki[1*], C. P. Providakis[1], C. E. Chalioris[2]

[1]*Technical University of Crete, Department of Applied Science, Chania, 73100, Greece*
[2]*Democritus University of Thrace, Department of Civil Engineering, Xanthi, 67100, Greece*
**mvoutetaki@yahoo.com*

Keywords: FRP-strengthened concrete, piezoelectric materials (PZT), damage repair, FEM.

Abstract

This study investigates the active control of the debonding procedure in dynamically loaded concrete members strengthened with Fibre-Reinforced-Polymer (FRP) materials using local smart piezoelectric actuators/sensors and electro-mechanical admittance concept. The proposed method is based on the estimation of the optimum electric voltage in order to give "secondary forces" with the same magnitude but with opposite effect to that caused to the damaged area of the adhesive-concrete interface of the FRP-strengthened concrete element. The results show that for the optimal voltage level the piezoelectric actuation eliminates the stress concentration at the debonding area of the FRP. Quantitatively, the normal tensile stresses at the critical concrete - FRP adhesive interface are reduced below the concrete tensile strength, which suggests an effective prevention of the FRP debonding.

1 Introduction

Repair and strengthening of damaged or inadequate civil infrastructures are challenging fields of study in engineering. Externally bonded FRP materials have been widely applied to strengthen existing structurally deficient concrete structures as an alternative to traditional heavy steel plate bonding techniques [1-4]. They have also been examined as Externally Bonded Reinforcement (EBR) to existing concrete members under various loading conditions such as flexure [5,6], shear [7,8] and torsion [9]. The primary goal of FRP is to improve the structural behaviour or/and to increase the ultimate capacity of the existing structures, which will in turn extend their service life. Although there is an extensive use of FRP materials as EBR, experimental results revealed that premature debonding failures of the FRP is usually exhibited before the potential full structural strength is achieved [10, 11]. It was proved that the FRP edge debonding initiation and development are usually closely related to the concrete crack propagation. Additionally, pre-existing defects such as air voids may be produced between the FRP and concrete surface during the FRP installation. These defects will also significantly impair the integrity of the strengthened structure. Since the FRP edge debonding prevents the ultimate capacity of the strengthened element from being utilized, it is crucial to be able to detect, identify and finally mitigate the initiation and progress of this debonding.

On the other hand, damage detection and Structural Health Monitoring (SHM) of existing structures is an important issue since crack initiation in critical structural components may lead to serious damages and potential catastrophic failures. Recent SHM systems which are

based on piezoelectric materials have been provided a promising approach in concrete structures, because these smart materials operate as both sensor and actuator and they can be easily surface-mounted on or embedded in the concrete member to be monitored [12]. However, due to the complex nature of the concrete microstructure, SHM of concrete structures still imposes many challenges, which can cause severe limitations on both the resolution and sensitivity of the signals observed. Unlike the usual SHM methods that operate in a passive manner, the active SHM techniques are capable of exciting the structure and in a prescribed manner can examine possible damage very quickly when and where required. Techniques that can detect damage in an active SHM fashion by using arrays of piezoelectric actuators/sensors have attracted a lot of attention from researchers. Typical examples include impedance-based, vibration-characteristic-based and Lamb-wave-based methods [13]. The impedance-based method was recently used to detect damage in concrete elements by using piezoceramic materials as actuators to generate high frequency vibrating waves and as sensors to detect the waves [14-16].

Further, several conventional non-destructive evaluation techniques have been proposed in order to detect and identify FRP edge debonding [17]. However, they are based on qualitative diagnostics and focuses on the identification of pre-existing defects and therefore, no information on debonding initiation and development is provided. Thus, it is imperative to develop a self-monitoring FRP retrofits to evaluate and control appropriately the edge debonding at both global and local levels in concrete infrastructures strengthened using EBR with FRP materials. A smart FRP retrofits system was firstly introduced by Rabinovitch [18, 19] where the prevention of the edge debonding in concrete beams strengthened with externally bonded FRP materials was investigated. Although, he theoretically demonstrated that the piezoelectric reduction of the edge stresses prevents the edge debonding failure and the avoidance of the overall global failure, he also concluded to the necessity of a more systematic approach for the design and use of the actuating/sensing piezoelectric system.

In a recent paper by Providakis et al. [20], the E/M admittance data are used to control the vibration response of a dynamically loaded structural component. In this study, the feasibility of the use of E/M admittance concept as a control strategy for the FRP edge debonging generated in the critical concrete-adhesive interface of FRP-strengthened concrete member under dynamic load is investigated. It can be considered as an extension of the work of Providakis and Voutetaki [21] by introducing the concept of E/M admittance in connection with the Finite Element Method (FEM) to produce a given E/M admittance signature of the healthy FRP retrofits. The proposed methodology leads to compute the optimum electric voltages, which give "secondary forces" with opposite effect to that caused to the edge debonded FRP strengthening strip by the imposed dynamic load.

2 Debonding of externally bonded FRP plates

Intensive research has been conducted on the performance of concrete members strengthened with EBR using FRP materials because they have many advantages over conventional strengthening methods. However, their advanced mechanical properties are achieved only when FRP rapture is obtained. In most of the examined cases FRP-strengthened concrete elements exhibit concrete fracture due to FRP over-reinforcing or premature debonding failure due to FRP delamination - cohesive failure through adhesive. In order to estimate the influence of the premature debonding failure of the FRP on the maximum potential tensile strength due to the fibre rapture, the rational model of Chen & Teng [11] is used. This model is based on fracture mechanics analysis using experimental data and is suitable for practical application in the design of FRP-to-concrete bonded plates. The developed stress and strain of FRP at bond failure ($\sigma_{f,deb}$ and $\varepsilon_{f,deb}$, respectively) can be estimated using the expression:

$$\frac{\sigma_{f,deb}}{f_{f,rupt}} = \frac{0.427\beta_p\beta_L}{\varepsilon_{uf}L_e} \Rightarrow \varepsilon_{f,deb} = \frac{0.427\beta_p\beta_L}{L_e} \tag{1}$$

where:

$f_{f,rupt}$: maximum tensile strength of FRP due to fibre rupture that equals to: $\varepsilon_{uf}E_f$,

ε_{uf}, E_f: FRP ultimate strain and modulus of elasticity, respectively,

L_e: effective FRP bond length that equals to: $L_e = \sqrt{\frac{E_f t_f}{\sqrt{f_c}}}$,

t_f, b_f, L_f: FRP thickness, width and bond length, respectively,

f_c: concrete compressive strength,

b_c: width of concrete member,

$$\beta_L = \begin{cases} 1 & L_f \geq L_e \\ \sin\frac{\pi L_f}{2L_e} & L_f < L_e \end{cases} \text{ and } \beta_p = \sqrt{\frac{2-b_f/b_c}{1+b_f/b_c}} \xrightarrow{b_f=b_c} \beta_p = 0.707$$

Figure 1 displays the flexural capacity ratio of the examined beam to the control concrete beam without FRP versus the midspan deflection for the cases of (a) a concrete beam without FRP, (b) the same concrete beam strengthened using EBR with FRP that exhibits premature debonding failure as it is calculated by equation (1) and (c) the same FRP-strengthened concrete beam that demonstrates an idealized flexural response of a perfectly bonded FRP. As it was expected, significant reduction of the ultimate capabilities of the beam is observed due to the premature FRP debonding failure.

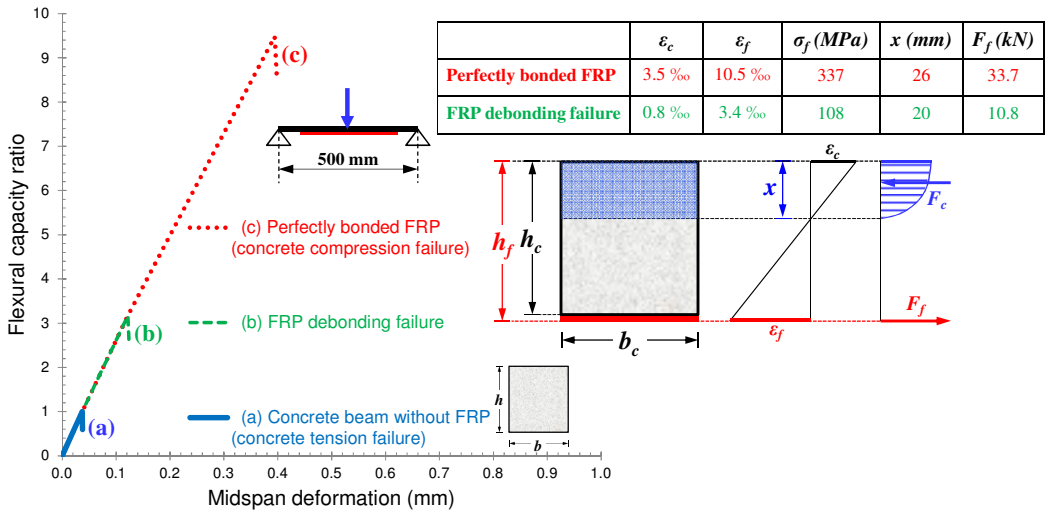

	ε_c	ε_f	σ_f (MPa)	x (mm)	F_f (kN)
Perfectly bonded FRP	3.5 ‰	10.5 ‰	337	26	33.7
FRP debonding failure	0.8 ‰	3.4 ‰	108	20	10.8

Figure 1. Influence of the FRP debonding failure to the ultimate flexural capacity of the simply supported concrete beam strengthened with externally bonded FRP plate (see also application in paragraph 5)

3 Finite element formulation

A FEM for dynamic analysis of piezoelectric material can be in written partition form as [20]:

$$\begin{aligned} [M_{uu}]\ddot{u} + [K_{uu}]u + [K_{u\varphi}]\Phi &= \{F\} \\ [K_{u\varphi}^T]u + [K_{\varphi\varphi}]\Phi &= \{Q\} \end{aligned} \tag{2}$$

where $[\mathrm{M_{uu}}]$ is a the kinematically constant mass matrix, $[\mathrm{K_{uu}}]$ is the elastic stiffness matrix, $[\mathrm{K_{u\varphi}}]$ is the piezoelectric coupling matrix, $[\mathrm{K_{\varphi\varphi}}]$ is the dielectric stiffness matrix, $\{\mathrm{F}\}$ is the mechanical force and $\{\mathrm{Q}\}$ is the electrical charge. For harmonic case the following matrix equations are derived:

$$\left(-\omega^2\begin{bmatrix}\mathrm{M_{uu}} & 0\\ 0 & 0\end{bmatrix}+\begin{bmatrix}K_{uu} & K_{u\phi}\\ K_{u\phi} & K_{\phi\phi}\end{bmatrix}\right)\begin{Bmatrix}\{\mathrm{u}\}\\ \{\Phi\}\end{Bmatrix}=\begin{Bmatrix}\{\mathrm{F}\}\\ \{\mathrm{Q}\}\end{Bmatrix} \tag{3}$$

where ω is the angular frequency. The response then can be obtained in the frequency domain for the displacements {u} and potential {Φ}, for a given charge or force excitation at a given angular frequency. Following the E/M admittance approach [19] when a unit voltage is applied to the piezoelectric layer of the finite element model of the piezoelectric patch the E/M admittance could be calculated at the patch electrode surfaces using the following equation. This piezoelectric patch can be considered as an Admittance Calculating Sensor (ACS) patch with the positive and negative electrodes located at its upper and lower, respectively, surfaces. In this way, the admittance can be easily calculated by calculating the ratio of the resulting current and the applied unit voltage. The resulting admittance *Y* is related to the total reaction charge on the piezoelectric ACS patch surfaces as:

$$Y=\frac{I}{V}=i\,\omega\,\Sigma Q_n \tag{4}$$

where ΣQ_n is the sum of the reaction charges resulted from the finite element analysis on all nodes belonging to the appropriate piezoelectric ACS patch. Conductance is the real part of the resulted admittance and susceptance is the imaginary part. These electrical "signatures" of the structure contain vital information concerning the phenomenological nature of the structural parameters (stiffness, damping and mass). The structural dynamic response corresponds to a unique pattern of the sharp peaks generated above the baseline electrical capacitive admittance in the admittance versus frequency plots.

4 Repair of debonded FRP plates using E/M admittance signature

This study is mainly an extension of the works of Providakis et al. [18]. It is focused to find out the required piezoelectric actuator input voltages to produce a desired E/M admittance signature of the healthy FRP retrofits at pre-selected locations of the vibrating structure. As first step, a given or known E/M admittance signature is used to define the desired E/M admittance signature $\overline{Y}^{*}(\omega_l)$ of the healthy FRP retrofits at specific ACS patch with ω_l being the frequency sampling point. The second step is to define the required input voltage to the piezoelectric actuators in order to produce the closest computed $\overline{Y}(\omega_l)$ to $\overline{Y}^{*}(\omega_l)$ at the same ACS patch. Thus, for an ACS patch *r*, the E_r optimization function, which describes the discrepancy between the E/M admittance computed from the finite element model and its desired counterpart of the model can be defined as:

$$E_r=[\overline{\mathrm{Y}}(\omega_1)-\mathrm{Y}^{*}(\omega_1)]^2,\quad l=1,...,n_f \tag{5}$$

where n_f is the number of frequency sampling points of interest and E_r is the optimization function. Equation (5) will not be equal to zero unless the structural matrices and the resulted

vibration response are capable of representing the desired healthy FRP retrofits status. Therefore, the basic objective of this approach is to update the input voltage of the piezoelectric actuators to represent the desired response by using an optimization technique to adjust the vibration response of the finite elements. The present problem can be considered as a nonlinear inverse problem that requires a proper optimization solution technique. The optimization toolbox of MATLAB ver. 2008b [22] environment based upon sequential search is employed to determine the required input voltages for the selected frequency range. The search for a fit is terminated when error E_r is considered minimum. Further, to describe the dynamic response of the host structure and piezoelectric patches, commercial software package COMSOL ver. 3.5b [23] is used to build and simulate the mathematical model.

5 Application

The feasibility of the optimal piezoelectric system to control the edge debonding in the critical concrete-adhesive interface of an FRP-strengthened concrete beam structure is examined in the following example. The geometry and mesh of the 3D model of a simply supported concrete beam strengthened with an externally bonded FRP plate is shown in Figure 2.

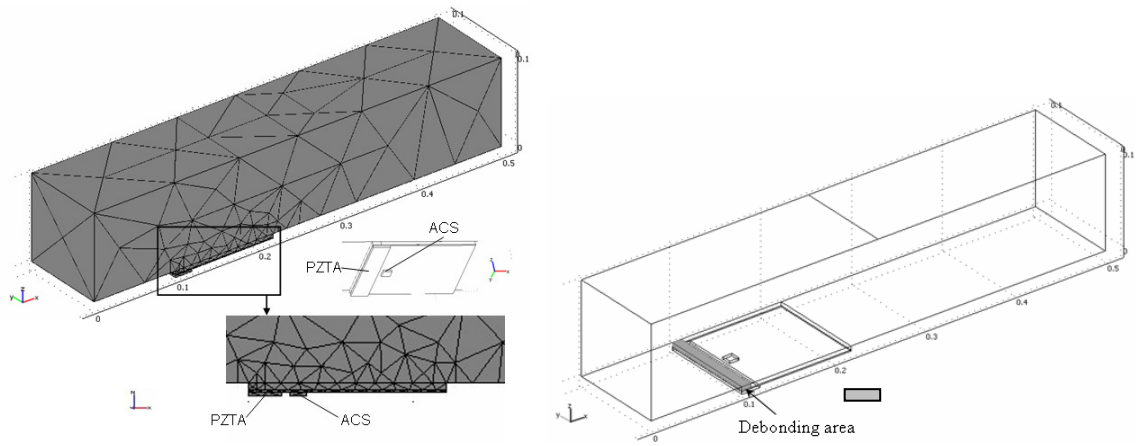

Figure 2. Geometry and 3D model of the FRP-strengthened concrete beam and the debonding area

Lead zirconate titanates (PZT), classified as piezoelectric materials are used as surface-mounted PZT Admittance Calculating Sensor (ACS) for the measure of the E/M admittance and PZT Actuator (PZTA) for the activation and the subsequent creation of appropriate forces to restore any observed debonding. The PZTA component spans the entire width of the FRP strengthening patch. In this model, the adhesive layer is modeled as a 3D linear orthotropic medium that resists shear and vertical normal stresses, while its in-plane rigidity is neglected. The concrete beam is modeled using classical 3D solid element deformation theory while the behavior of the active layers is governed by the piezoelectric constitutive equations. The mechanical, electrical and E/M properties of the used materials are presented in Table 1.
It is also assumed that perfect bonding exists at the interfaces with the adjacent components: the concrete beam, the FRP plate, or the surface active layer. Input voltage can be applied on the top nodes of the PZTA and admittance sensor ACS and zero voltage is assigned for all the bottom nodes of both the PZTA and sensor to simulate the grounding operation. The beam is vibrating under an excitation of $-100e^{i\omega t}$ applied at the upper surface of the midspan. Figure 2 also presents the simulation of the debonding area of 10 mm in length while it is extended across the entire width of the concrete beam specimen. The debonding area is modeled by taking a 90% reduction on the original value of the healthy adhesive layer's modulus of elasticity.

	Concrete	FRP plate	Adhesive layer	Damaged adhesive layer
Elastic modulus (GPa)	22.5	32	3.8	0.038
ρ (Density Kg/m^3)	2400	2000	1310	1310
ν (Poison ratio)	0.21	0.20	0.21	0.21
Tensile strength (MPa)	2.0	2400		
PZT	S_E (1/Pa) compliance matrix: $\begin{bmatrix} 16.5e-12 & -4.78e-12 & -8.45e-12 & 0 & 0 & 0 \\ -4.78e-12 & 16.5e-12 & -8.45e-12 & 0 & 0 & 0 \\ -8.45e-12 & -8.45e-12 & 20.7e-12 & 0 & 0 & 0 \\ 0 & 0 & 0 & 43.5e-12 & 0 & 0 \\ 0 & 0 & 0 & 0 & 43.5e-12 & 0 \\ 0 & 0 & 0 & 0 & 0 & 42.6e-12 \end{bmatrix}$			
	d (C/N) coupling matrix: $\begin{bmatrix} 0 & 0 & 0 & 0 & 741e-12 & 0 \\ 0 & 0 & 0 & 741e-12 & 0 & 0 \\ -274e-12 & -274e-12 & 593e-12 & 0 & 0 & 0 \end{bmatrix}$			
	ε_{rT} relative permittivity: $\begin{bmatrix} 3130 & 0 & 0 \\ 0 & 3130 & 0 \\ 0 & 0 & 3400 \end{bmatrix}$ and ρ = 7500 kg/m^3 (density)			

Table 1. Mechanical, electrical and E/M properties of the used materials.

The E/M admittance was extracted at the upper surface of ACS component at each predefined frequency step and then a qualitative analysis was performed to track the changes in the real part of the signature. Figure 3a shows the extracted E/M admittance signature for both the debonding and healthy case of the investigated FRP-strengthened concrete beam for a frequency range of 720 up to 800 Hz. The sharp peaks in the real part of E/M admittance almost correspond to the structural resonant frequencies. The edge debonding of the FRP composite causes a regular downward shifting of the resonance peak (up to 14%) which suggests a stiffness reduction.

After the activation of the PZTA actuator with the optimum electrical voltage at the frequency range of 720 up to 800 Hz, one can clearly observed in Figure 3b that the actuator causes a shifting of the resonance peaks to reach the original healthy FRP retrofits E/M admittance signature, which in turn suggests a restoration of the debonding area.

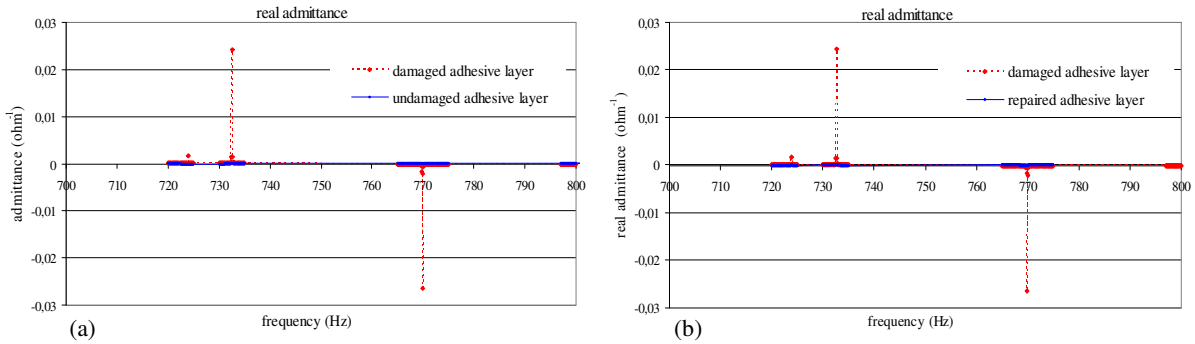

Figure 3. E/M admittance versus frequency

Figure 4 shows the surface distribution of the vertical normal stresses at the critical concrete-adhesive interface under the determined optimal voltage level of the PZTA actuator at

frequency 732.6 Hz. The results clearly show that for the optimal voltage level the PZTA eliminates the stress concentration at the debonding area. Quantitatively, although the stresses at this specific frequency are not totally eliminated, the electrical actuation at the optimal voltage level reduces the normal tensile stresses at the critical concrete-adhesive interface below the tensile strength of the concrete. Although in damaged cases the normal tensile stresses at the critical concrete-adhesive interface are close to the tensile strength of the concrete in repaired cases the normal tensile stresses have been decreased by far from the above values. This has as a result the reduction of extension of debonding of the FRP retrofit.

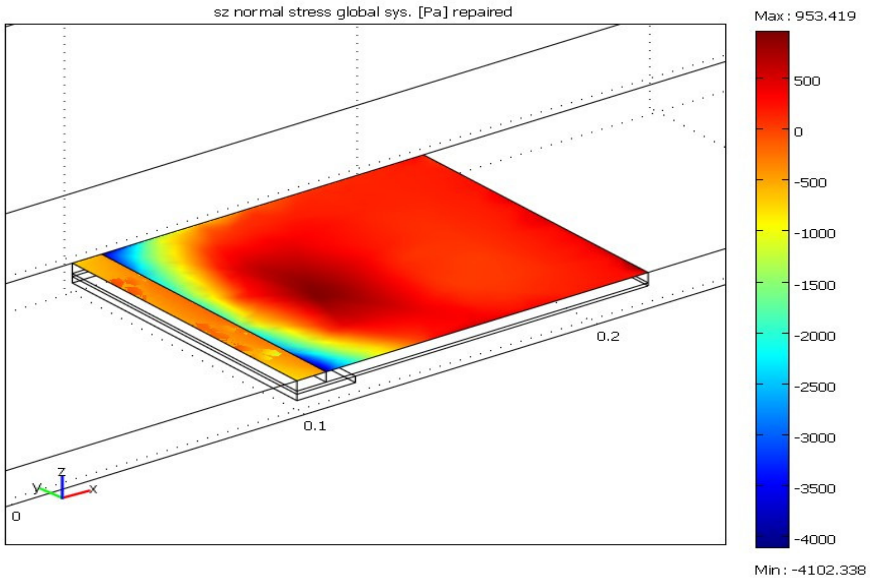

Figure 4. Surface distribution of the vertical normal stresses

6 Concluding remarks

This paper presents an E/M admittance-based active edge debonding repair approach of a vibrating structure using finite element analysis. The design consists of integrated PZT actuators and piezoelectric ACS patches attached to the vibrating host structure. An active edge debonding repair scheme for solving nonlinear optimization problem is proposed to obtain a desired healthy structure's E/M admittance signature at specific PZT locations, through matching the numerically computed and desired E/M admittance on the ACS piezoelectric transducer.

References

[1] ACI Committee 440, 440.2R-02: *Design and construction of externally bonded FRP systems for strengthening concrete structures*. American Concrete Institute, Farmington Hills, MI (2006).

[2] Triantafillou T.C. Strengthening of structures with advanced FRPs. *Progress in Structural Engineering and Materials*, **1**, pp. 126-134 (1998).

[3] Karayannis C.G., Sirkelis G.M. Strengthening and rehabilitation of RC beam-column joints using carbon-FRP jacketing and epoxy resin injection. *Earthquake Engineering and Structural Dynamics*, **37**, pp. 769-790, (2008).

[4] Tavakkolizadeh M., Saadatmanesh H. Strengthening of steel-concrete composite girders using carbon fiber reinforced polymers sheets. *Journal of Structural Engineering, ASCE*, **129**, pp. 30-40 (2003).

[5] Teng J.G., Zhang J.W., Smith S.T. Interfacial stresses in reinforced concrete beams bonded with a soffit plate: A Finite Element Study. *Construction and Building Materials*, **16**, pp. 1-14 (2002).
[6] Karayannis C.G., Sirkelis G.M. *Behaviour of flexural R/C beams reinforced with carbon FRP tested in cyclic loading* in "Proceedings of the of the *2nd Hellenic Conference on Earthquake Engineering and Technical Seismology*, (in Greek), Vol. B, Thessaloniki, Greece, pp. 417-424, (2001).
[7] Chalioris C.E. *Shear performance of RC beams using FRP sheets covering part of the shear span* in "Proceedings of the *1st International Conference on Concrete Repair*, Vol. 2, St-Malo, Brittany, France, pp. 809-816, (2003).
[8] Triantafillou T.C. Shear strengthening of reinforced concrete beams using epoxy-bonded FRP composites. *ACI Structural Journal*, **95**, pp. 107-115 (1998).
[9] Chalioris C.E. Torsional strengthening of rectangular and flanged beams using carbon fibre-reinforced-polymers - Experimental study. *Construction and Building Materials*, **22**, pp. 21-29, (2008).
[10] Karayannis C.G., Chalioris C.E. *Experimental investigation of the contribution of bonded C-FRP jackets to shear capacity of RC beams* in "Role of Concrete in Sustainable Development", Thomas Telford Ltd, London, Dundee, United Kingdom pp. 689-696 (2003).
[11] Chen J.F., Teng J.G., Anchorage strength models for FRP and steel plates bonded to concrete. *Journal of Structural Engineering, ASCE*, **127**, pp. 784-791 (2001).
[12] Providakis C.P., Voutetaki M.E. *PZT control of edge debonding in dynamically loaded concrete structures strengthened with composite materials* in "Proceedings of the *ECCOMAS Thematic Conference on Computational Methods in Structural Dynamics and Earthquake Engineering (COMPDYN 2009)*, Rhodes, Greece, (2009).
[13] Song G., Gu H., Mo Y.L., Hsu T.T.C., Dhonde H. Concrete structural health monitoring using embedded piezoceramic transducers. *Smart Material Structures*, **16**, pp. 959-968 (2007).
[14] Ayres J.W., Lalande F., Chaudhry Z., Rogers C. Qualitative impedance-based health monitoring of civil infrastructures. *Smart Material Structures*, **7**, pp. 599-605 (1998).
[15] Soh C.H., Tseng K.K., Bhalla S., Gupta A. Performance of smart piezoceramic patches in health monitoring of a RC bridge. *Smart Material Structures*, **9**, pp. 533-42 (2000).
[16] Park G., Cudney H.H., Inman D.J. Impedance-based health monitoring of civil structural components. *Infrastructure Systems*, **6**, pp. 153-160 (2000).
[17] Kaiser H., Karbhari V.M. Non-destructive testing techniques for FRP rehabilitated concrete - A critical review. *Materials and Product Technology*, **21**, pp. 349-384 (2004).
[18] Rabinovitch O. Piezoelectric control of edge debonding in beams strengthened with composite materials: Part I - Analytical modeling. *Composite Materials*, **41**, pp. 525-546 (2007).
[19] Rabinovitch O. Piezoelectric control of edge debonding in beams strengthened with composite materials: Part II - Failure criteria and ptimization. *Composite Materials*, **41**, pp. 657-677 (2007).
[20] Providakis C.P., Kontoni D.-P.N., Voutetaki M.E. Development of an electromechanical admittance approach for application in the vibration control of intelligent structures. *Smart Materials and Structures*, **16**, pp. 275-281 (2007).
[21] Providakis C.P., Voutetaki M.E. Electromechanical admittance - based damage identification using Box-Behnken design of experiments. *Tech Science Press, SDHM Structural Durability and Health Monitoring*, **3**, pp. 211-227 (2007).
[22] MATLAB 2008b, *The Mathworks Inc. Users Guide*, www.mathworks.com, U.S. (2008).
[23] COMSOL 3.5a Ltd., *Comsol Multiphysics Modeling 3.5a. Users Guide*, London (2008).